Paper ID ILASS08-4-6

BINARY WATER DROPLET COLLISION UNDER VARIOUS GASEOUS CONDITIONS TYPICAL FOR NUCLEAR REACTORS

Christophe Rabe[1], Pierre Berthoumieu[2], Jeanne Malet[1], François Feuillebois[3]

[1]Institut de Radioprotection et de Sûreté Nucléaire
DSU/SERAC
Laboratoire d'Etudes et de Modélisation en Aérodispersion et Confinement,
BP 68, 91192 Gif-sur-Yvette Cedex, France

[2]Office National d'Etudes et de Recherche Aérospatiales
Heterogeneous, Multiphase Flows Unit
Aerodynamics and Energetics Models Departement
BP 4025-2, avenue Edouard Belin 31055 Toulouse Cedex 4, France

[3]Laboratoire de Physique et Mécanique des Milieux Hétérogènes - UMR CNRS 7636
École Supérieure de Physique et de Chimie Industrielles,
10 rue Vauquelin 75231 Paris Cedex 05, France

ABSTRACT
Droplet collisions for Weber number from 5 to 120 have been studied. Experiments have been performed with same diameter water droplets between 220 to 450 µm for different impact parameters. Gas conditions directly surrounding binary droplet collision have been modified in order to study the gas properties influence on collision outcomes. Coalescence, reflexive and stretching separation have been recorded in ambient conditions whereas bouncing only appeared when gas density or viscosity changes. A large amount of pictures leads to numerous data which provide collision outcomes mapping at pressures of 1.5, 2.5, 3 and 3.5 bar. Droplet collisions have also been completed in an air-helium environment in order to simulate hydrogen accumulation. Results obtained in both cases are presented according to gas viscosity and density and show the influence of these variable on collision issues.

INTRODUCTION AND OBJECTIVE

Spray systems are emergency devices designed for preserving the containment integrity in case of a severe accident in a Pressurized Water Reactor. These systems are used to prevent overpressure, to cool the enclosure atmosphere, to remove fission products and to enhance the gas mixing in case of hydrogen presence in the reactor containment. The efficiency of these sprays depends partially on the evolution of the droplet size distribution in the containment, due to gravity drag forces, heat and mass transfers with the surrounding gas, and droplets collision. Spray systems in reactor applications are composed of over 500 interacting water droplet sprays with droplets diameters range from 100 to 1000 µm. They are used under pressure (2-3 bars) at temperature between 20 and 60 °C, and under gaseous mixture composed of water steam, hydrogen and air.

In this paper, special care will be given to the water droplet coalescence. According to the literature (see Orme [1]), five collisions regimes can be pointed out: coalescence with minor deformation, bouncing, coalescence with major deformation, reflexive and stretching separation. In most studies, the collision process is characterized by three parameters: the Weber number *We*, the impact parameter *I* and the diameter ratio Δ, which depend on the large droplet diameter d_l, the small droplet diameter d_s, the droplets relative velocity u_r, the liquid density ρ_{liq}, the surface tension coefficient σ and the dimensional impact parameter x (see Figure 1):

$$We = \frac{\rho_{liq} d_s u_r^2}{\sigma} \qquad I = \frac{2x}{d_l + d_s} \qquad \Delta = \frac{d_s}{d_l}$$

These parameters are used to determine the transition curves between all binary collision outcomes domains.

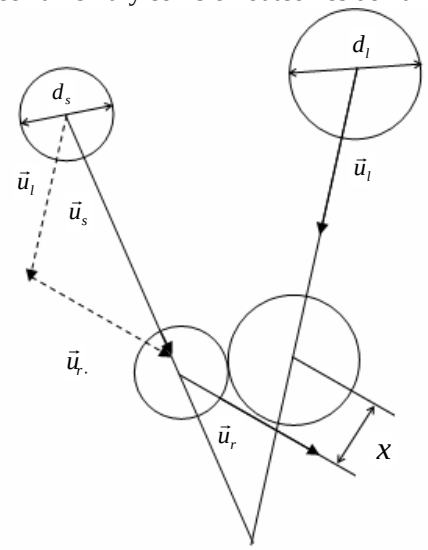

Figure 1 Geometric impact parameter x for droplet collision

According to Orme [1], most studies concern fuel droplets for Weber number lower than 250. Only few studies concern water droplets. Ashgriz and Poo [2] worked, under ambient conditions, with droplets between 100 and 500 µm diameter, diameter ratio of 0.5, 0.75 and 1, Weber number range of 1 to 100 and impact parameter between 0 and 1, which

corresponds to low droplet velocities and collision angles. Nevertheless, recent studies, (Quian and Law [3]), showed that droplet collision behaviour depends also on ambient conditions like pressure, temperature, relative humidity and gas properties such as density or viscosity. However, no data exist for hypothetical nuclear reactor accident typical conditions. The purpose of the present work is thus to extend the previous results on water droplet coalescence by studying a wider range of parameters typical for reactor conditions.

EXPERIMENTAL SETUPS

To investigate droplets collision, an experimental method, widely used in many studies like the ones of Ashgriz and Poo [2] or Estrade [7], consists in producing two calibrated droplet streams with converging trajectories. Binary droplets collision could thus be periodically obtained and recorded. Droplets stream generators had been realized at the ITLR (Institut fur Thermodynamik Luft und Raumfahrt, Stuttgart). They are constituted by a steel tube ended by an iridium plate with a calibrated hole. A piezoelectric cell surrounds the upward extremity of the tube and allows the mechanical perturbation of the liquid jet according to electrical signal modulation. Instability also growing along the jet, in relation with Rayleigh theory, leaves to the break-up of the water filament and to the development of droplets with same characteristics (velocity, diameter, direction). The experimental set-up which has been developed at the IRSN allows the production of water droplets with diameters from 200 to 700 µm. Droplet velocities used are between 1 and 19 $m.s^{-1}$, and droplet stream collision angles between 10 and 95°. Collision observation is realized by two cameras which record respectively the front and the lateral views, as shown on Figure 2.

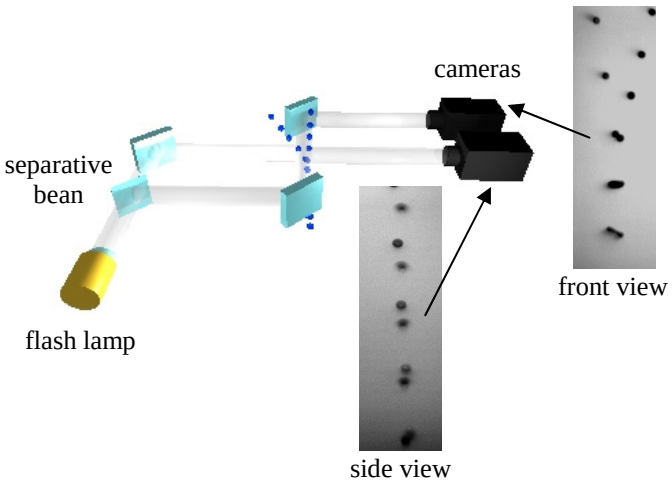

Figure 2. Periodic droplet collision recording system.

A shadowgraphic process is used to record a large number of collisions by lighting the scene with a very short stroboscopic flash (about 150 ns). Picture sequences are collected and transmitted to a computer which is in charge of image processing. An image sequence treatment process, developed for this purpose in JAVA with the ImageJ software, is then applied to calculate droplet velocities, impact parameter and Weber number. This experimental postprocessing is quite well adapted to achieve a large amount of data which provide a complete mapping of droplet collision outcomes in a large field of Weber number. A global effort had also been carried out to evaluate the uncertainties of measurements. It had been assess to reach a maximum of 8 % for Weber number and 10 % for impact parameter especially due to the pixel size of the CCD camera.

Three different experimental campaigns had been carried out in order to evaluate the occurrence of many collision outcomes under various ambient gaseous atmospheres. First set of experiments was done under atmospheric conditions on the IRSN device that has been built up on an optical board to avoid parasite vibrations affecting droplet generation.

A second set of experiments have next been completed with a similar device in a pressurised enclosure of $2.7x10^{-3}$ m^3, at ONERA.

In this work, binary droplet collisions have been performed under various pressures up to 2.5 bar.

At last, gas viscosity influence have also been analysed by recording droplet collisions in an air-helium mixture atmosphere. This was done by injecting a controlled mixture in the vessel enclosing the IRSN set-up. A necessary time to ensure a homogeneous concentration is needed. Various helium concentrations were used to modify the gas properties, as density and viscosity.

Results obtained will be described in the following section.

RESULTS IN ATMOSPHERIC CONDITIONS

Before investigating reactor condition influence on droplet collision, such as gas pressure or hydrogen influence simulated here by helium, a complete description of the collision mechanisms in ambient conditions would be given. These ones have been exhibited by proceeding to the collision outcomes mapping according to Weber number and impact parameter. First results obtained, in the range of Weber number between 25 and 100, were used to evaluate the measurement uncertainties and to identify the different collision regimes occurring with water droplet, in ambient conditions.

Three different outcomes, described in the work of Ashgriz and Poo [2] as coalescence, reflexive separation and stretching separation, have been pointed out. Pictures of these mechanisms are given on Figure 3. As the coalescence leads to the merging of the two initial droplets, separation processes could produce many satellites droplets. Nevertheless, reflexive separation diverges from stretching by its capacity to merge completely the colliding droplets. A disk is first formed due to counteractive flows and tends then to oscillate before breaking up. In case of stretching separation, droplets keep their initial trajectories while exchanging a small amount of fluid. The “liquid bridge” also established between the drops, extends and gets thinner just before breaking up too. Its break-up, in relation with Rayleigh’s theory, could lead to the production of smaller droplets.

The occurrence field (according to *We* and *I*) of the three outcomes, has been delimeted by Ashgriz and Poo [2] for water droplets and is represented on Figure 4. The uncertainty, only mentioned at time in previous studies, has also been plotted on the figure.

In order to extend these results, obtained during experimental set-up checking, a large set of experiments with same diameter droplets (d = 450 µm, Δ = 1) has been conducted.

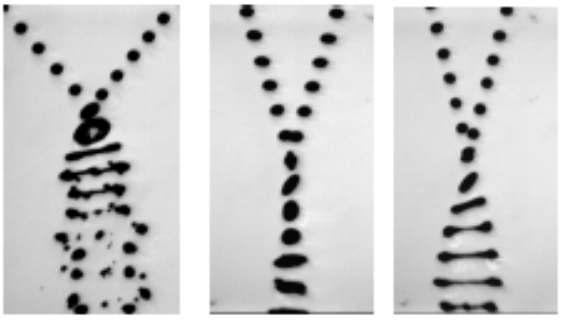

Reflexive Separation | Coalescence | Stretching Separation

Figure 3. Droplet collision outcomes under ambient conditions.

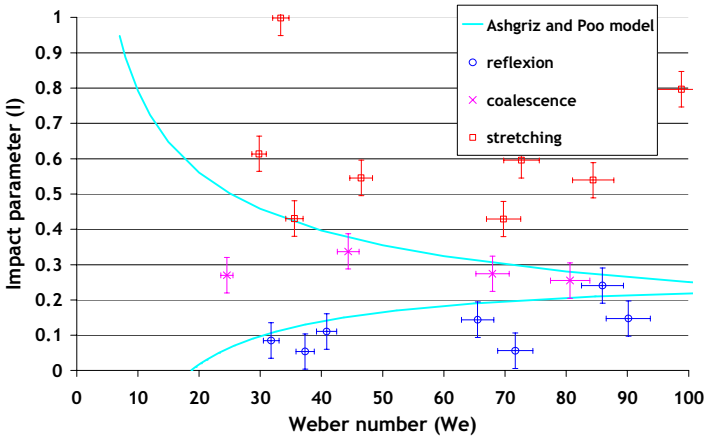

Figure 4. Error evaluation plotted on collision outcomes.

The range of Weber number studied has thus been enlarged to a maximum value of 280. Moreover, thanks to the use of the experimental setup developed at the IRSN, an increase of the measures number realized for each sequence recorded leads to a large amount of values obtained, as it could be seen on Figure 5. Indeed for fixed liquid flow rate, droplet size and Weber number, many sequences recorded provide collisions pictures for a large number of different Impact parameter. This could be explained by the fact that droplet streams disintegration process tends to be modified slightly with time. Orange curve represents the transition between coalescence and stretching separation (C/S) determined by Ashgriz and Poo [2]. This curve has been plotted using the following equation:

$$We_{C/S} = \frac{4\left(1+\Delta^3\right)^2\left[3(1+\Delta)(1-x)\left(\Delta^3\Phi_s+\Phi_l\right)\right]^{\frac{1}{2}}}{\Delta^2\left[\left(1+\Delta^3\right)-\left(1-I^2\right)\left(\Phi_s+\Delta^3\Phi_l\right)\right]} \quad (1)$$

Where Φ represents the droplets volume fraction which interact each other:

$$\Phi_s = \begin{cases} 1-\frac{1}{4\Delta^3}(2\Delta-\tau)^2(\Delta+\tau) & \text{for } h>\frac{1}{2}d_s \\ \frac{\tau^2}{4\Delta^3}(3\Delta-\tau) & \text{for } h<\frac{1}{2}d_s \end{cases} \quad (2)$$

And

$$\Phi_l = \begin{cases} 1-\frac{1}{4}(2-\tau)^2(1+\tau) & \text{for } h>\frac{1}{2}d_l \\ \frac{\tau^2}{4}(3-\tau) & \text{for } h<\frac{1}{2}d_l \end{cases} \quad (3)$$

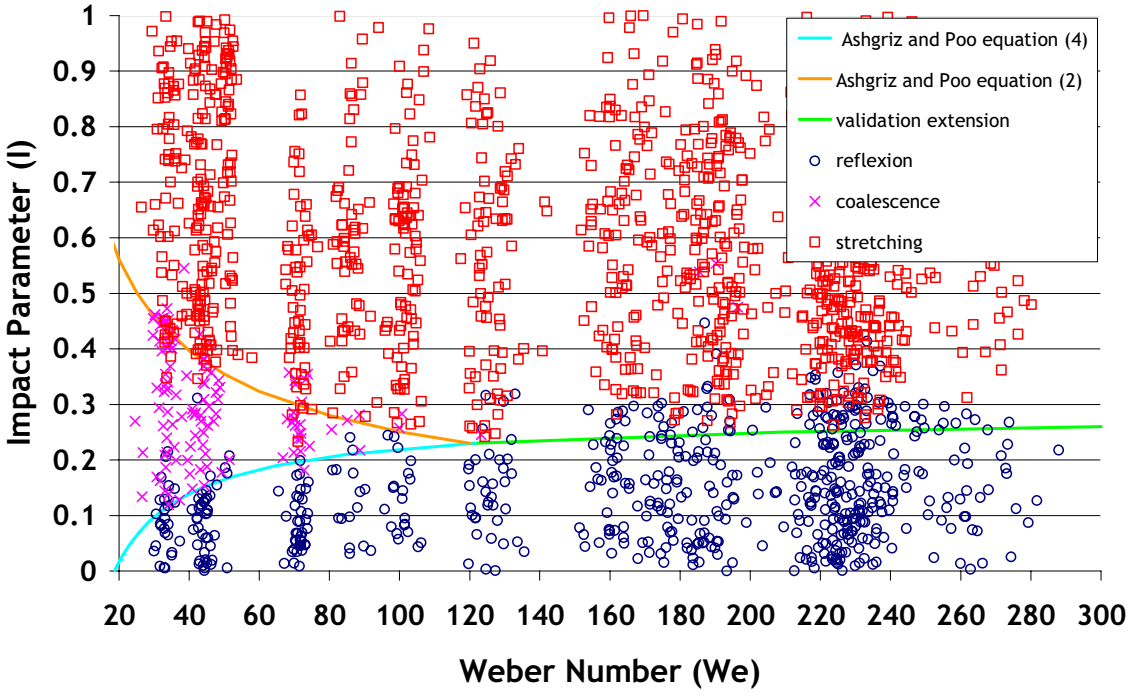

Figure 5. Experimental results compared to Ashgriz and Poo [2] model for water droplets of same diameter d = 450 µm, Δ = 1.

where $\tau = (1-I)(1+\Delta)$ and $h = \frac{1}{2}(d_l + d_s)(1-I)$ (4)

h represents the height of the interacting volumes. Δ is the diameter ratio and x the impact parameter detailed on Figure 1. Blue curve designs the transition between reflexive separation and coalescence (R/C). It has been explained by this equation:

$$We_{R/C} = \left[\frac{3\left(7(1+\Delta^3)^{\frac{2}{3}} - 4(1+\Delta^2)\right)\Delta(1+\Delta^3)^2}{(\eta_2 + \Delta^6\eta_1)} \right] \quad (5)$$

Here

$$\eta_1 = 2(1-\zeta)^2\left(1-\zeta^2\right)^{\frac{1}{2}} - 1 \quad (6)$$

$$\eta_2 = 2(\Delta-\zeta)^2\left(\Delta^2-\zeta^2\right)^{\frac{1}{2}} - \Delta^3 \quad (7)$$

And $\xi = \frac{1}{2}x(1+\Delta)$ (8)

The two last expressions (defining the critical Weber number between observed outcomes) are coming from the Ashgriz and Poo [2] work. They were obtained by considering the energy balance between kinetic and surface tension forces. For reflexion / coalescence transition, Ashgriz and Poo [2] considered that separation occurs if kinetic energy excesses 75% of the final drop surface energy. Regarding stretching / coalescence boundaries, kinetic energies of drops interacting volume are compared to the surface energy of the approximate cylinder formed during collision.

As it clearly appears on Figure 5, results obtained for Weber number under 120 are in good agreement with the Ashgriz and Poo [2] model.

An increase of droplet velocities and collision angles leads to enlarge the previous field of Weber number studied by Ashgriz and Poo [2]. According to this process, a maximum value of 280 had been reached. It appears that for We>120, only stretching and reflexion outcomes could be detected.

An extension of Ashgriz and Poo [2] model for critical *We* between reflexion and coalescence has also been plotted on Figure 5 to sketch a transition curve between stretching and reflexive separation. Even if this modelling seems to be at first an adapted approximation, it appears to undervalue slightly the reflexive separation field in comparison with the stretching domain.

RESULTS AT VARIOUS PRESSURIZED ATMOSPHERES

The enclosure used for droplet collision under pressure is principally composed of two main parts, one corresponding to the location of droplet generators (at the top) coupled with micrometric displacement systems, and the other one to the vessel where droplets collision is acting. As vessel section is of only 0.003 m² with a height smaller than 0.03 m, a small air leak have to be adjusted in order to evacuate the humide air without getting down the pressure. According to this process, a maximum humidity of 25% have been kept in the enclosure during the whole experimental campaign.

Water droplets with same diameter of 220 µm have been used to complete collision outcomes mapping at different pressures. Relative velocities between 1 to 5 m/s were applied to examine outcomes in the field of *We* smaller than 60 until pressure do not exceed 2 bar. For the hightest considered P = 3.5 bar , Weber number up to 120 were studied. Results have been ploted on Figure 7, 8, 9,10.

A first observation, in regard to these graphs, is the occurence of the bouncing regime as pressure increases (i.e for P ≥ 1.5 bar), whereas it could not been observed under ambient conditions for We>120 (see Figure 5).

Bouncing phenomenon, that is observed on Figure 6, comes out due to the presence of a thin gas film, between droplets, which could not be evacuate. Pressure applied by approching droplets on the gas film is not high enough to get it thinner and evacuate it completely. Thus, as droplets could not get closer, Van Der Vaals forces, which are preponderant for smallest distances, could not take place to promote droplets coalescence. As a consequence, the gas film separating droplets could not be broken and becomes trapped between the two particles. Droplets are then bouncing on each side of the gas film.

Moreover, it could be seen on Figure 6 that droplets shapes are modified just after the collision which could be assumed as an partially inelastic shock. This phenomenon is due to the droplets kinetic energies which are converted in inner energies. This inner energy variation could be observed according to the surface deformation of the droplets. Indeed, surface tension forces contribute to the inner energy excess evacuation by modifying droplet surface area. This is what happens when droplets are oscillating a few time after collision, in order to evacuate the shock energy and to recover a spheric stable shape.

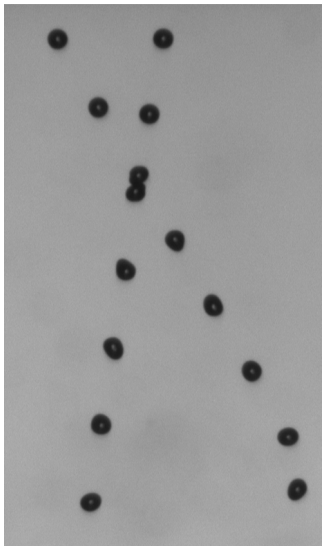

Figure 6. Picture of bouncing outcome ($P = 2\ bar, We = 20.2, I = 0.63$).

It has been assumed by many authors that bouncing regime depends on ambient conditions like gas properties. When gas pressure grows, an increase of gas density is also carried out. As a consequence, it could clearly be noticed that bouncing regime is promoted when the pressure grows up on the four following graphs.

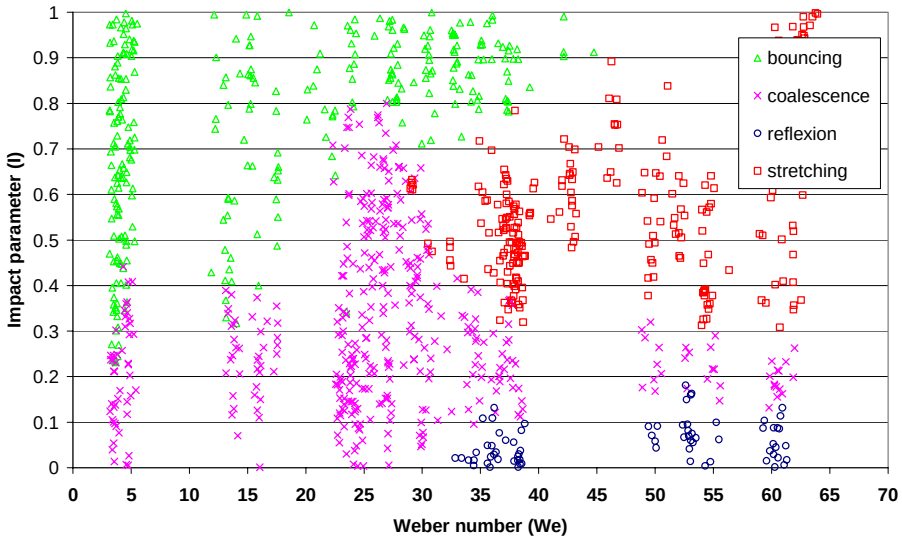

Figure 7. Experimental results of different outcomes for collisions of water drops of same diameter (d = 220 µm, Δ = 1, P = 1.5 bar).

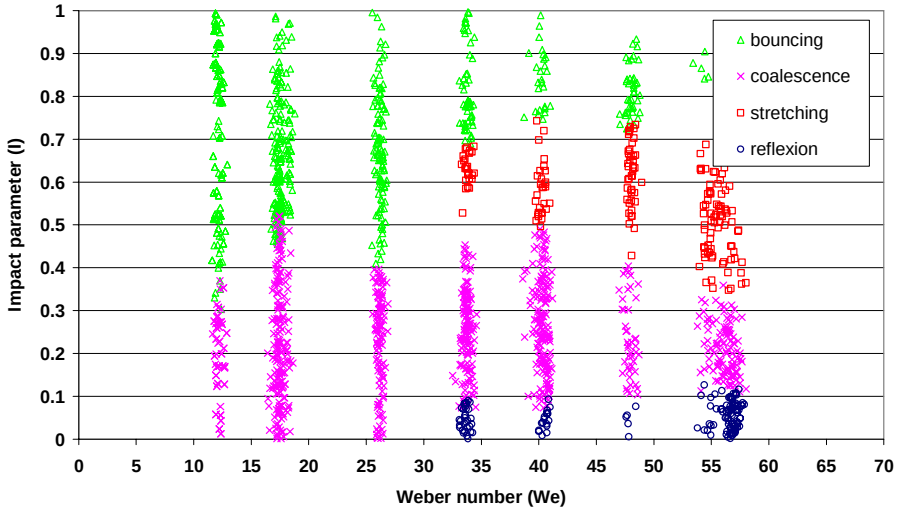

Figure 8. Experimental results of different outcomes for collisions of water drops of same diameter (d = 220 µm, Δ = 1, P = 2.5 bar).

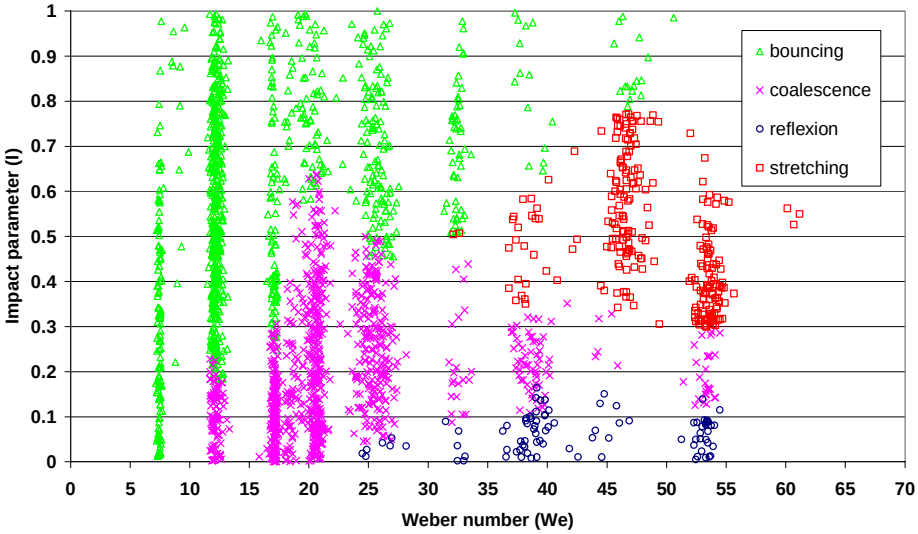

Figure 9. Experimental results of different outcomes for collisions of water drops of same diameter(d = 220 µm, Δ = 1, P = 3 bar).

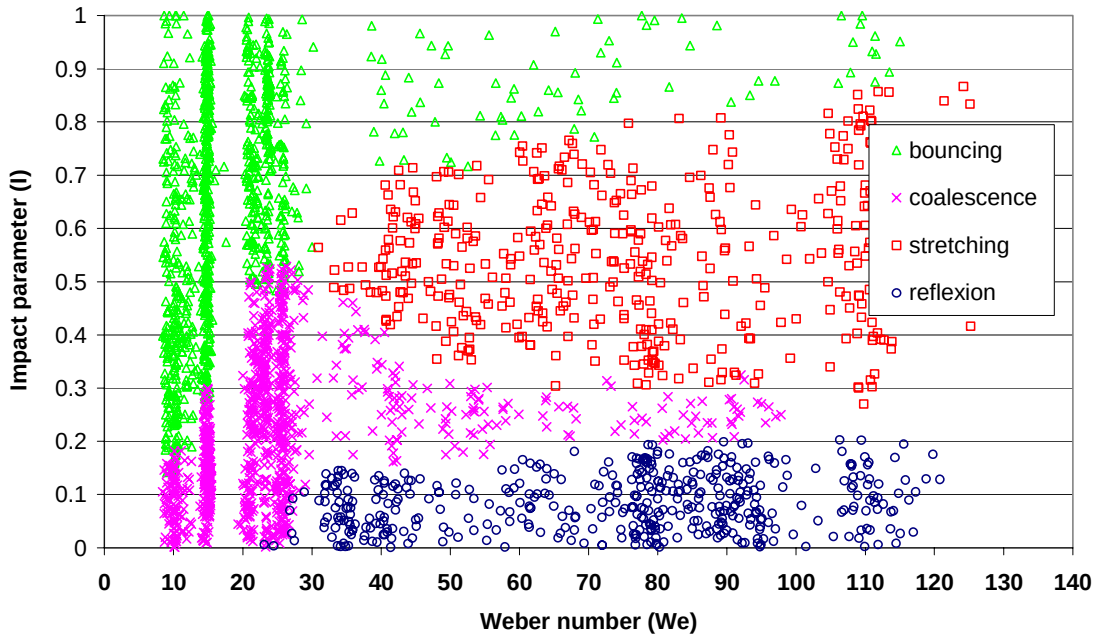

Figure 10. Experimental results of different outcomes for collisions of water drops of same diameter(d = 220 µm, Δ = 1, P = 3.5 bar).

It could be assumed that these phenomena could depend on the gas film inertia which is directly affected by the density. Thus, so as to expel this film, droplets need to apply an important pressure on it. This pressure is then directly linked to droplets velocities and thus with Weber number. This is why droplet velocity, as Weber number, is assumed to play a role on coalescence outcome appearing. The evolution of gas density according to pressure in the enclosure is summarized in Table 1.

Table 1. Pressure and gaz density in relation with figures

Figures	**Total Pressure (bar)**	**Gas Density ρ_{gaz} (kg/m^3)**
Figure 5	1	1.18
Figure 7	1.5	1.77
Figure 8	2.5	2.94
Figure 9	3	3.52
Figure 10	3.5	4.11

Graphics presented above attest of the bouncing evolution with gas density. Locations of the three outcomes exhibited at ambient pressure (coalescence, stretching separation and reflexive separation) are the same: these regimes do not seem to be affected by the pressure evolution.

As experiments carried out at ambient pressure did not provide any bouncing, a relative pressure increase of only 0.5 bar leads to a bouncing region appearance on the *We / I* outcomes mapping (see Figure 7). This graph also shows that bouncing domain is bounded by an impact parameter value of 0.4 for We < 10 and does not extend after We < 40.

When the pressure reaches 1.5 bar (see Figure 8) bouncing tends to occur for higher value of *We* up to 55-60. Coalescence domain also seems to be replaced by bouncing for *We* values in the field of 25.

On Figure 9, namely for P = 2 bar, only bouncing outcome has been reported for We < 10 which leads to coalescence disappear as it was observed for lower pressures. Moreover, it can be seen that for impact parameter values higher than 0.6, and for *We* value in the range of 40, bouncing substitutes for stretching separation.

At last, with an ambient pressure of 3.5 bar in the vessel (Figure 10), bouncing outcome has been recorded in the whole field of *We* studied. Indeed, if bouncing is preponderant for *We* values under 10, it appears to be of importance also for *We* up to 120, i.e. for impact parameter above 0.9.

Bouncing outcome has been shown by pressure increase. Its domain clearly extends when density increases. These observations are in good agreement with the ones of Quian and Low [3]. Results they obtained with a nitrogen environment at 2.7 bar are sensibly the same than those obtained here with air at 2.5 bar. Moreover, more collision data between 1 and 2.5 bar had been collected here and complete the gap between 1 and 2.7 bar in their study. These data are also in good accordance regarding to the bouncing outcome development.

RESULTS UNDER AIR-HELIUM MIX ATMOSPHERE

Influence of viscosity on collision outcome has been investigated and results are presented in this section. Further experiments have been conducted by customizing the experimental set-up built up at the IRSN. This was performed by confining the set-up in a large transparent Plexiglas® enclosure. Various helium-air concentrations mixtures have been introduced directly closest to the droplets collision point.

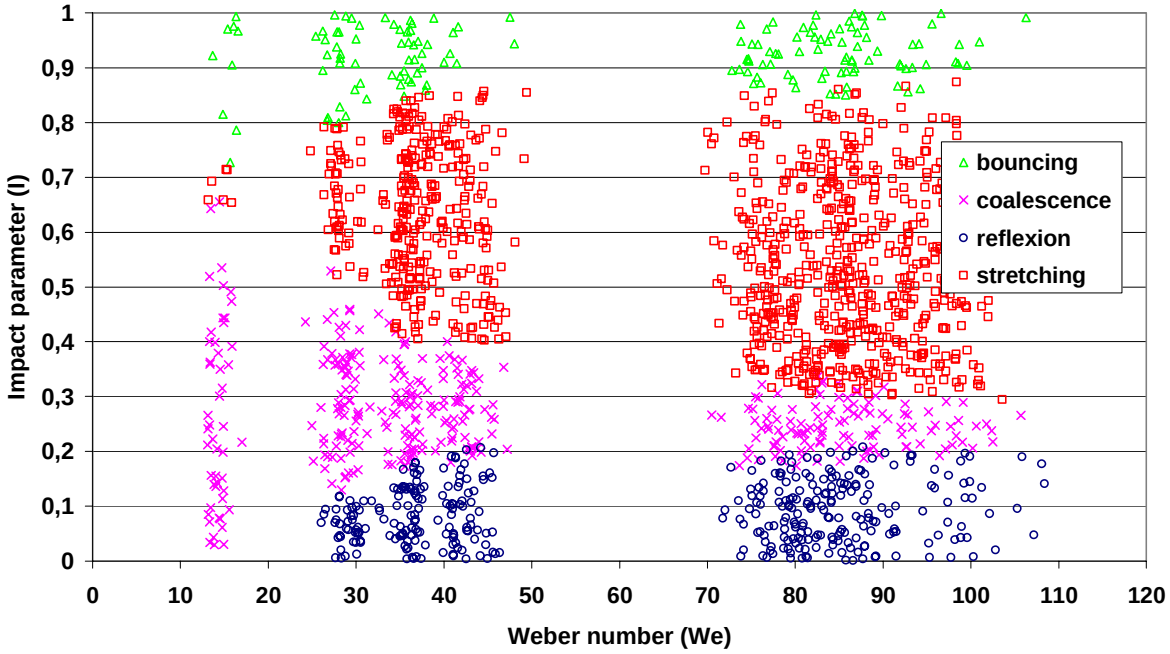

Figure 11. Experimental obtained regions of different outcomes for air helium mixture (d = 300 µm, Δ = 1, C_{0He} = 50 %).

A large plate was also disposed in front of the injection location in order to avoid droplet stream disturbance due to the injected gas velocity. Three different gas mixtures have been tested and used in the enclosure during droplets collision recording. For each campaign, only gas components (air and helium) concentration in the mixture were modified. Concentrations of the three mixtures (10% vol, 50% vol and 85% vol of helium) have been evaluated using a mass spectrometer (Fabstar) that has previously been calibrated on specific air-helium mixture bottles.

Moreover, before collisions recording, gas mixture was injected during three removal time (about one hour for a gas flow rate of 56 $L.min^{-1}$) in order to ensure 95% of the concentration of the injected mixture in the enclosure.

In the following section, only results obtained with a 50% vol air-helium mixture are presented on Figure 11 as this case corresponds to the gas density obtained at P = 1.5 bar. Droplets with same diameters of 300 µm have been used to carry on binary collisions which have shown the occurrence of reflexion, stretching, coalescence and bouncing outcomes for Weber number included between 10 and 110. Boundary limits between coalescence regime and separation ones seem to be the same than those achieved in ambient conditions (see Figure 5). Nevertheless, bouncing outcome is observed for low *We* where its domain extends till impact parameter of 0.75, as it was not detected under air conditions at atmospheric pressure. Additionally, it is observed that bouncing is also of importance for *We* up to 110 when impact parameter is above 0.85. This noticeable situation has to be considered to take into account gas properties influence. Indeed, as bouncing regime is more significant at low *We* for a pressurised air environnement at 1.5 bar, it appears to be extended over *We* of 55 in an air-helium mixture. This phenomenon could be assumed to be relevant of the gas viscosity increase. As viscosity does not change largely when the pressure is not drastically intensified, it is modified by the helium introduction. These modifications have been summarized in Table 2.

Table 2. Gas density and viscosity in relation with figures.

Figures	**Gas Viscosity μ_{gas} (µPa s)**	**Gas Density ρ_{gas} (kg/m^3)**	**Total Pressure (bar)**
Figure 5	18.71	1.18	1
Figure 7	18.71	1.77	1.5
Figure 11	26.83	1.77	1

It clearly comes into sight that even if gas density is lower for air-helium mixture than for pressurised air, bouncing could be observed in the two situations. Gas viscosity, which is larger in air-helium mixture, seems then to play an important role on bouncing outcome development. Indeed, because of viscosity increase, gas film trapped between droplets could not be expelled sufficiently fast and leads then to bouncing.

CONCLUSION

Current models for binary droplets collision outcomes description, especially for water droplets, are limited to ambient conditions. In the field of nuclear plants safety investigations, new results are necessary to understand droplet size evolution in spraying systems due to coalescence or separation process under a pressurized environment or under various hydrogen concentrations. The present investigation will help to establish semi-empirical models delimiting boundary domains of the various collision outcomes in the frame of reactor environment conditions. Thanks to the two different experimental set-ups detailed in the present paper, dedicated to pressure effects and to helium concentration influence, four collision issues were observed. Coalescence, reflexive and stretching separation domains, which already appeared under atmospheric conditions do not exhibit significant modifications whereas bouncing (that is not detected under ambient conditions) appears. Indeed, pressure increase and thus gas density lead to an extension of the bouncing domain that stands for coalescence at low Weber number. These conclusions correspond to those

formulated by Quian and Low [3] who worked with higher environment pressures. Nevertheless, the present study also constitutes an extension of their study by increasing data they had collected.

Moreover, bouncing also exhibits a gas viscosity dependency as it takes place over a large part of high impact parameter values in the whole field of Weber number studied. This observation is coming from data obtained in a helium environment, as for Quian and Low [3], but with different pressure and concentration. An important conclusion of this work is thus that gas viscosity is assumed to play a large role in bouncing occurrence, even if its variation is not very important. These conclusions would influence the bouncing modelling development as they act entirely in the inertial effects consideration necessity. Some more investigations at higher pressure or with a very high gas viscosity have to be considered to enhance this modelling.

NOMENCLATURE

Symbol	Quantity	SI Unit
C_{0He}	Helium concentration	-
d	Droplet diameter	m
d_l	Large droplet diameter	m
d_s	Small droplet diameter	m
h	Interacting height	m
I	Non dimensional impact parameter	-
P	Pressure	bar
u_l	Large droplet velocity	m/s
u_r	Relative velocity	m/s
u_s	Small droplet velocity	m/s
We	Weber number	-
$We_{C/S}$	Critical Weber number between coalescence and stretching	-
$We_{R/C}$	Critical Weber number between reflexion and coalescence	-
x	Impact parameter	m
ρ_{air}	Air density	kg/m^3
ρ_{gas}	Gas mixture density	kg/m^3
ρ_{He}	Helium density	kg/m^3
ρ_{liq}	Liquid density	kg/m^3
σ	Surface tension	N/m
μ_{air}	Air dynamic viscosity	Pa.s
μ_{gas}	Gas mixture dynamic viscosity	Pa.s
μ_{He}	Helium dynamic viscosity	Pa.s

REFERENCES

[1] M. Orme, Experiments on droplet collisions, bounce, coalescence and disruption, *Prog. Energy Combust. Sci* vol. 23, pp. 65-79, 1997.

[2] N. Ashgriz and J.Y. Poo, Coalescence and Separation in Binary Collision of Liquid Droplets, *J. Fluid. Mech.*, vol. 221, pp. 183-204, 1990.

[3] J. Quian and C.K. Law, Regimes of coalescence and separation in droplet collision, *J. Fluid. Mech*., vol. 331, pp. 59-80, 1997.

[4] P.R. Brazier-Smith, S.G. Jennings and J. Latham, The interaction of falling water drops: Coalescence, *Proc. Roy. Soc. London*, vol. A226, pp. 393-408, 1972.

[5] N. Roth, M. Rieber and A. Frohn, High energy head-on collision of droplets, ILASS-Europe, Toulouse, France 1999.

[6] N. Roth, C. Rabe, B. Weigand, F. Feuillebois, and J. Malet, Droplet Collision at High Weber Number, ILASS-Europe, Mugla, Turkey, Sept.2007.

[7] J.P. Estrade, Etude expérimentale et numérique de la collision de gouttelettes, Ph.D. thesis, Ecole Nationale Supérieure de l'Aéronautique et de l'Espace, France, 1999.